

Hyun-Joo Kim
Sunok Oh
Myeong Hee Moon

Department of Chemistry, Yonsei
University, Seoul, Korea

Original Paper

Hollow-fiber flow/hyperlayer field-flow fractionation for the size characterization of airborne particle fractions obtained by SPLITT fractionation

Hollow-fiber flow field-flow fractionation (HF FIFFF) was applied for the separation and size characterization of airborne particles which were collected in a municipal area and prefractionated into four different-diameter intervals (>5.0, 2.5–5.0, 1.5–2.5, <1.5 μm) by continuous split-flow thin (SPLITT) fractionation. Experiments demonstrated the possibility of utilizing a hollow-fiber module for the high-performance separation of supramicron-sized airborne particles at steric/hyperlayer operating mode of HF FIFFF. Eluting particles during HF FIFFF separation were collected at short time intervals (~ 10 s) for the microscopic examination. It showed that particle size and size distributions of all SPLITT fractions of airborne particles can be readily obtained using a calibration and that HF FIFFF can be utilized for the size confirmation of the sorted particle fraction during SPLITT fractionation.

Keywords: Airborne particle / Hollow-fiber flow field-flow fractionation / Hyperlayer separation / Size characterization / SPLITT

Received: November 2, 2005; revised: December 5, 2005; accepted: December 6, 2005

DOI 10.1002/jssc.200500420

1 Introduction

Fine particulate matter in air is one of the major concerns in environmental science since it carries potentially toxic chemicals, which can be transported to human by inhaling and can cause respiratory diseases. Since smaller particles have a larger surface area to adsorb more of toxic chemicals (polychlorinated dibenzo-*p*-dioxins and furans (PCDD/Fs), polycyclic aromatic hydrocarbons (PAHs), heavy metals, *etc.*) than larger ones, particle sizes and the distribution of airborne particles are important parameters in dealing with air pollution [1, 2]. In relation to the origin of the fine particles, information on particle size distribution (PSD) and the size-dependent level of pollutants is of interest. For such a multidimensional analysis, an accurate size fractionation of particles into a certain diameter range must be achieved first, and proper methods to analyze size distribution and pollutants should be applied together.

Determination of particle size and the size distribution of environmental particles has been typically made with

Correspondence: Professor Myeong Hee Moon, Department of Chemistry, Yonsei University, Seoul 120-749, Korea.
E-mail: mhmoon@yonsei.ac.kr.
Fax: +82 2 364 7050.

Abbreviations: GSF, gravitational SPLITT fractionation; HF FIFFF, hollow-fiber flow field-flow fractionation; PS, polystyrene; PSD, particle size distribution; SPLITT, split-flow thin

the use of a Coulter Multisizer [3–5], photon correlation spectroscopy (PCS) [6, 7], microscopy [8, 9], differential mobility particle sizers (DMPS) [10, 11], and condensation particle counters (CPC) [12]. A fast and accurate measurement of the size distribution of airborne particles is not simple to obtain due to its heterogeneity in particle density, shape, and solubility. The first two techniques mentioned above are very simple in operation but they are accurate only when PSD is narrow. While the microscopic work provides accurate size measurement, it requires considerable amount of time and effort. The last two techniques (DPMS, CPC) are good only for aerosol nanoparticles.

Hollow-fiber flow field-flow fractionation (HF FIFFF), a variant of FIFFF techniques, was first described in a few papers on separation of spherical latex standard particles [13, 14], and recently it has been gaining interest as an efficient separation technique for particles [15, 16], proteins [17–19], and cells [20, 21]. Unlike the conventional FIFFF channel system having a rectangular channel design, HF FIFFF is operated in a cylindrical channel utilizing a hollow-fiber membrane module which is very simple in assembly and disposable. In HF FIFFF, particles are separated by the control of axial flow moving along the fiber axis and the radial flow exiting through the pores of the HF membrane wall. When radial flow is applied to particles in the HF FIFFF channel, particles are driven toward the vicinity of the fiber wall. However, par-

ticles larger than 1 μm are lifted against the fiber wall by hydrodynamic lift forces and they reach equilibrium states some distances apart from the wall according to the difference in particle sizes. When axial flow is applied to particles located at different equilibrium heights against the fiber wall, particles will migrate at different velocities. In case of separating particles larger than typically 1 μm (in some cases, this value is as small as 0.4–0.8 μm in typical flow FFF [22]), particle elution follows the principle of hyperlayer mode of separation in which a large particle is lifted further away from the wall than the small one due to the action of hydrodynamic lift forces, and thus a large particle is eluted earlier than a small one [16, 23, 24]. In recent studies, HF FIFFF has been applied to the investigation of membrane effect on resolution and selectivity of hyperlayer separation of polystyrene (PS) standard particles [16] and for the characterization of supramicron-sized cells and bacteria [21]. Since particle retention in FIFFF is regardless of density or mass, separation of particles in HF FIFFF is influenced by the hydrodynamic radius only. Therefore, particle size or size distribution can be obtained if a proper calibration in hollow-fiber flow/hyperlayer field-flow fractionation (HF FI/HyFFF) is established with standard particles [17, 21].

In a previous study [25], fractionation of airborne particles into several diameter fractions (>5.0, 2.5–5.0, 1.5–2.5, <1.5 μm) was successfully carried out by using gravitational split-flow thin (SPLITT) fractionation (GSF) yielding a few tenth of grams for each diameter interval and the resulting fractions were examined for the determination of PCDD/Fs. GSF is a continuous and rapid particle separation technique using two different flow streams in a thin rectangular channel having two different inlets and outlets [25–30] under a gravitational force. In GSF, particles larger than or equal to a certain diameter (cut-off diameter) are eluted through one exit of the channel while smaller particles are eluted through the other exit of the channel. Therefore, particle fraction of a narrow-diameter interval can be achieved by subsequent fractionations of collected particles by decreasing the cut-off diameter. Adjustment of cut-off diameter can be made with the fine control of the flow rates at the two outlets.

In this study, HF FI/HyFFF was applied to characterize GSF fractions of airborne particles. This is the first application of HF FI/HyFFF toward the separation and characterization of environmental particles. Compared to the use of a conventional rectangular flow FFF channel system, it provides a low cost in channel assembly and eventually a disposability which can reduce fear of sample carry-over problems caused by possible adhesion of particles to the channel membrane. In the previous work [25], particle size confirmation of GSF fractions made by microscopic examination, it took enormous time and

effort. By utilizing HF FI/HyFFF, it is demonstrated that GSF fractions of airborne particles can be separated at a high speed and the PSDs can be readily obtained. Average diameter of each GSF fraction by electron microscopy was compared with the value calculated from HF FI/HyFFF calibration.

2 Experimental

Hollow-fiber membrane used in this study was polyacrylamide (PAN) having a dimension of 1.0 mm \times 1.4 mm (ID \times OD) with a molecular weight cut-off of 30 000 from Chemicore (Daejeon, Korea). The HF module was prepared by inserting a 24-cm long HF membrane into a Teflon tubing (OD \times ID: 3.2 \times 1.6 mm) as shown in Fig. 1 and the connection between the fiber and the exterior housing was made without applying glue by using hand-tight ferrules only. The detailed method was described in the previous study [31].

The HF channel and the system assembly are illustrated in Fig. 1. A Model 930 HPLC pump from Young-Lin Scientific (Seoul, Korea) was utilized for the delivery of carrier solution. The flow pathways during the focusing/relaxation procedure and during separation are expressed as dotted and solid lines, respectively. During focusing/relaxation mode (dotted line connection at both three-way and four-way valves), flow from the pump is divided

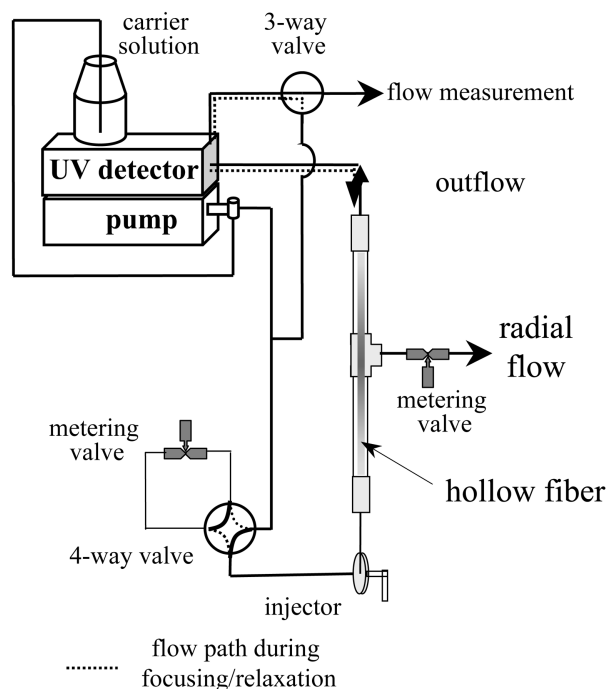


Figure 1. Configuration of the HF FIFFF system. The dotted line connections represent the flow direction during the focusing/relaxation process and the solid line pathways for the elution mode.

into two parts: one toward the injector, a model 7125 loop injector from Rheodyne (Cotati, CA, USA), and the other leading to the outlet of HF. Flow rate ratio for the two directions was set as 1:9 (the inlet vs. outlet) by adjusting the fine metering needle valve from Crawford Fitting (Solon, OH, USA), connected at the four-way valve. At this stage, particle suspension was injected into the HF channel through the injector, and particles were expected to be focused at a position of 0.1 L (total length of HF). After 2 min and 20 s, which is the delivery time between the injector and the fiber inlet, both valves were switched to obtain the flow configuration indicated by the solid line configuration and the entire flow was delivered to the fiber inlet for sample elution. In order to control radial flow rate, another metering valve was used at the end of the radial flow outlet. Eluted particles were monitored at 254 nm by a Model 720 UV detector from Young-Lin Scientific. Data were recorded with Autochro-Win software from Young-Lin.

Carrier solution was made with ultrapure water ($>18\text{ M}\Omega$) by adding 0.1% FL-70, a mixture of ionic and nonionic surfactant [32] from Fisher Scientific (Firlawn, NJ, USA), with 0.02% sodium azide as a bactericide. The solution was filtered with a membrane filter (pore size: $0.45\text{ }\mu\text{m}$) before use.

Standard particles were PS latex spheres having nominal diameters of 8.020, 4.991, 3.004, and $2.013\text{ }\mu\text{m}$ (referred to as 8, 5, 3, and $2\text{ }\mu\text{m}$ hereafter) from Duke Scientific (Palo Alto, CA, USA) except the $8\text{ }\mu\text{m}$ standard that was obtained from Fluka (Buchs/Schweiz, Germany).

The airborne particle sample used in this study was collected on the roof of the College of Science building at Yonsei University by using a high-volume air sampler, Model HV-1000s from Sibata Scientific Technology, (Tokyo, Japan). Details of particle collection from the air and the fractionation of raw airborne particles by GSF into four size fractions (>5.0 , $2.5\text{--}5.0$, $1.5\text{--}2.5$, and $1.5\text{ }\mu\text{m}$) were reported in the previous work [25]. Electron micrographs of the four GSF fractions were adopted from [25] with permission and are shown in Fig. 2. During HF FI/HyFFF separation of GSF fraction of airborne particles, eluting particles were collected at time intervals of 10–12 s. Collected particles were examined by a Model JSM-5610 field emission scanning electron microscope from Jeol (Tokyo, Japan), and the average diameter of each narrow size fraction of airborne particles was measured.

3 Results and discussion

It was recently demonstrated that the hyperlayer separation of supramicron-sized particles by HF FIFFF can be achieved at a high speed, with resolution analogous to that obtained by a conventional rectangular flow FFF channel [15]. In the current study, HF FI/HyFFF was applied for the size characterization of airborne particles which were previously fractionated by GSF into four different-size fractions (>5.0 , $2.5\text{--}5.0$, $1.5\text{--}2.5$, $<1.5\text{ }\mu\text{m}$) [25]. In that study, particle size in each GSF fraction was measured by electron microscopy. It was found that each fraction contained more than 80% of particles in number, which belonged to the expected diameter range cal-

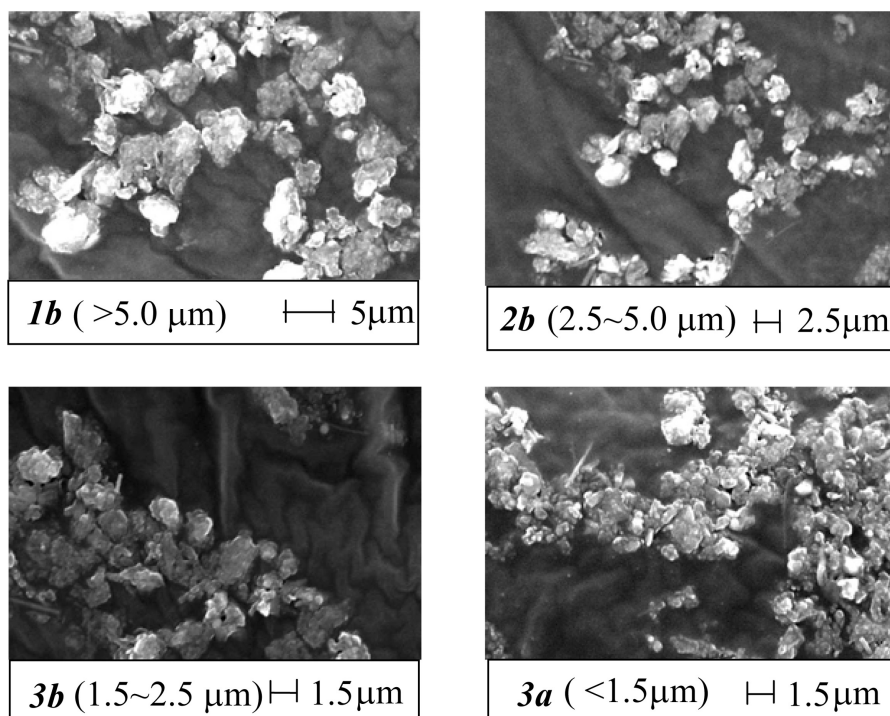


Figure 2. Electron micrographs of four pre-fractionated GSF fractions of airborne particles with permission from [25]. Expected diameter range of each GSF fraction is given by GSF theory.

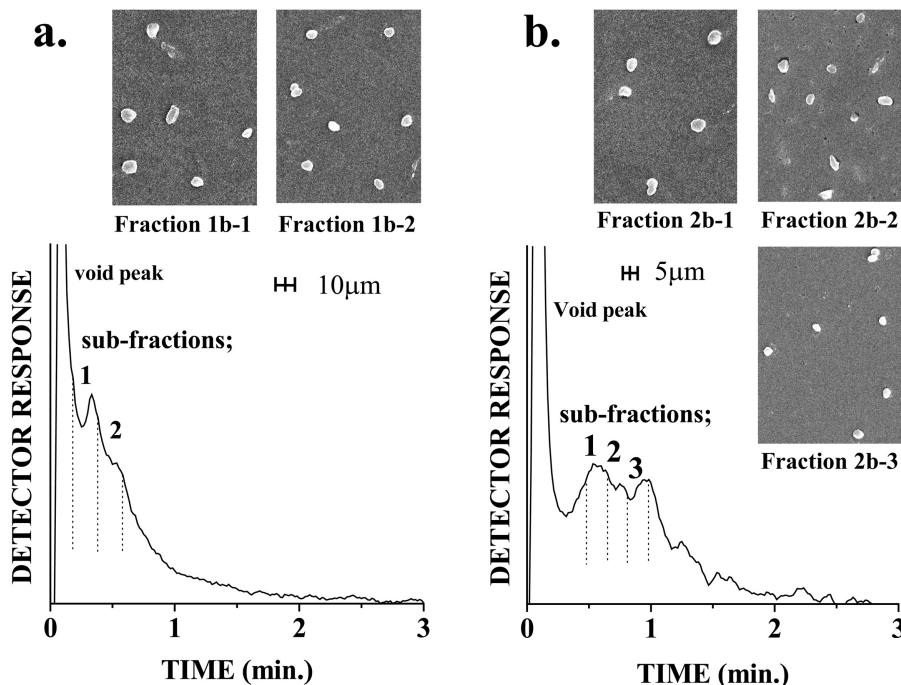


Figure 3. HF FI/HyFFF fractograms of the GSF fraction-1b (a) and -2b (b) of airborne particles along with electron micrographs of HF FI/HyFFF subfractions. Flow rates were $\dot{V}_{\text{rad}} = 0.60$ mL/min and $\dot{V}_{\text{out}} = 3.4$ mL/min.

culated by GSF theory. Figure 2 represents micrographs of the GSF fractions of airborne particles shown in [25] (some of the electron micrographs were adapted with permission). These fractions were subjected to HF FI/HyFFF separation for measuring PSD. Figure 3 showed the HF FI/HyFFF fractograms of (a) the GSF fraction 1b (>5.0 μm of an expected diameter range) and (b) the fraction 2b (2.5–5.0 μm) obtained at a radial flow rate, \dot{V}_{rad} , of 0.60 mL/min and an outflow rate, \dot{V}_{out} , of 3.4 mL/min. While Fig. 3a appeared with a relatively fast eluting peak right after the void peak, Fig. 3b showed a peak retained longer in the channel. This supported that the two GSF fractions had clearly different size distributions from each other. During the HF FI/HyFFF separation, eluted particles were collected within narrow time intervals (10–12 s) for confirming that average particle size decreased as subfraction number increased. Microscopic observation of the subfractions collected at the end of the hollow-fiber channel showed that the particles of the subfraction 1b-2 appeared to be smaller than those of 1b-1. This trend was clearly shown in the separation of the GSF fraction 2b in Fig. 3b. It is represented that the particles were separated by the hyperlayer operation mode of flow FFF since particles were eluted with decreasing size.

For the calculation of particle size and size distribution, a calibration run was performed with PS latex standards at the same flow rate condition used in Fig. 3. Figure 4 shows the separation of four PS standards (8, 5, 3, and 2 μm in diameter) achieved within 2 min, and the resulting calibration curve, a plot of $\log t_r$ versus $\log d$, in the inserted plot. The relationship between the retention

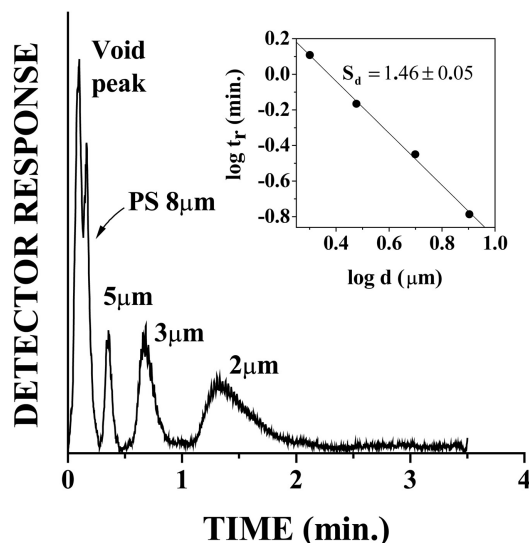
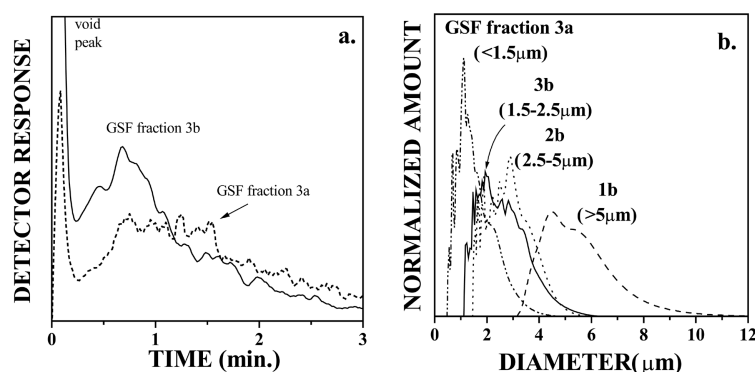


Figure 4. HF FI/HyFFF separation of polystyrene latex standards obtained. Run conditions were the same as used in Fig. 3. The inset shows the calibration plot of $\log t_r$ vs. $\log d$ for calibration.

time and particle diameter can be expressed as $\log t_r = -S_d \cdot \log d + \log t_{r1}$ where S_d is the diameter-based selectivity ($S_d = |d \log t_r / d \log d|$) representing the fractional increase of retention time with the change in diameter at logarithmic scale, and the t_{r1} represents the retention time of a unit diameter [16]. Calibration parameters were as following: $S_d = 1.46 \pm 0.05$ and $t_{r1} = 3.52 \pm 0.04$ min, with a correlation coefficient of 0.999 ($n = 3$). The selectivity value in this run was analogous to the values obtained

Table 1. Average diameter values measured from HF FI/HyFFF fractions of each GSF fraction and the corresponding diameter interval expected from a calibration run

GSF fraction No.	HF FI/HyFFF fraction No.	Collected time interval (min)	Diameter interval from calibration (μm)	Measured av. diameter (μm)
1b	1	0.18–0.38	7.66–4.59	6.26 ± 0.43
	2	0.38–0.58	4.59–3.44	4.81 ± 0.39
2b	1	0.48–0.65	3.91–3.18	3.88 ± 0.33
	2	0.65–0.81	3.18–2.74	3.41 ± 0.38
	3	0.81–0.98	2.74–2.40	2.91 ± 0.21
3b	1	0.48–0.65	3.91–3.18	2.82 ± 0.26
	2	0.65–0.81	3.18–2.74	2.51 ± 0.36
	3	0.81–0.98	2.74–2.40	2.13 ± 0.22
3a	1	0.65–0.81	3.18–2.74	1.91 ± 0.31
	2	0.81–0.98	2.74–2.40	1.52 ± 0.35
	4	1.15–1.31	2.15–1.97	1.03 ± 0.24

**Figure 5.** Superimposed (a) HF FI/HyFFF fractograms of the GSF fractions 3b and 3a, and (b) the particle size distributions of GSF fractions.

with an earlier study with HF FI/HyFFF [16]. Based on the calibration, the expected diameter range of each HF FI/HyFFF subfraction was calculated and compared with the measured average diameter value from the microscopic examination reported in Table 1. It appeared that the average particle size measured from subfractions of the GSF fraction 1b agreed well with the expected diameter interval from the calibration; however, those of subfractions 2b-2 and -3 were slightly larger than each expected diameter interval. But this deviation was not seriously large. However for GSF fractions of smaller sizes, 3b and 3a, the observed average diameter values of subfractions were smaller than the values expected from the calibration. As examined by SEM pictures, airborne particles did not appear as perfectly spherical in shape. Since nonspherical particles were reported to have a higher steric/hyperlayer effect [33], particles of the fractions 3b and 3a were expected to be eluted earlier than spherical particles of equivalent size. This deviation will result in the calculation of average diameter and PSD larger than actual values.

Figure 5 showed the (a) HF FI/HyFFF fractograms of both GSF fractions (3b and 3a) and (b) the resulting PSDs for all four GSF fractions. PSD was obtained by converting the

retention time of each fractogram into diameter values using the calibration parameters explained at the above. From Fig. 5b, the fractions 1b and 2b appeared to contain some undersized particles, which were the main source of contamination during GSF. However, PSDs of the fractions 3a and 3b appeared to shift toward the larger-diameter scale to some degree due to the deviation caused by the early elution of nonspherical particles. Data in Table 2 represented the number percentage of each fraction obtained by SEM and average diameter values obtained with SEM and HF FI/HyFFF measurements. Average diameter value by FFF calculation represents the average value of the PSD curve, which is based on surface area distribution. Since the average diameter value from SEM measurements is the number average value, a direct comparison between the two methods gives just qualitative indications. To obtain number distribution of PSD, the effect of light scattering on the extinction coefficient must be considered as it was reported in the literature [34]. This may be integrated in the future for the accurate size characterization by HF FI/HyFFF. Neither it may be overlooked the possibility that some particles can be disaggregated into very small ones and dissolved in solutions during the process of transferring them into liquid phase. This can be a possible shortcoming of the current

Table 2. Average diameter of GSF fractions of airborne particles measured from HF FI/HyFFF and electron microscopy (EM)

GSF fraction No.	Expected diameter range (μm)	Number percentage (%)		Average diameter (μm) \pm SD	
		$>d_c$	$<d_c$	SEM ^{a)}	HF FIFFF ^{b)}
GSF-1b	>5.0	85.5	14.5	6.3 ± 1.3	5.53 ± 2.42
GSF-2b	2.5–5.0	78.7	21.3	3.0 ± 0.7	2.88 ± 2.06
GSF-3b	1.5–2.5	84.2	15.8	1.8 ± 0.3	2.62 ± 2.15
GSF-3a	<1.5	8.8	91.2	1.0 ± 0.3	1.59 ± 1.32

a) Based on number average.

b) Based on area distribution of particle surface.

technique since FIFFF separation uses aqueous solution in most cases.

In this study, it was demonstrated that HF FI/HyFFF can be applied to the size characterization of supramicron-sized environmental particulates and the applied technique can be incorporated for the fast confirmation of diameter distribution of SPLITT fractions during continuous SPLITT fractionation of particulate materials. In the current calibration run, the lower limit of particle sizes that can be separated in HF FI/HyFFF appear to be as $2 \mu\text{m}$ in the case of PS. However, if a proper run condition is selected, this can be extended down to about $0.4 \mu\text{m}$ as it was observed in an earlier study [16] Since the hollow-fiber separation module can be made inexpensively, it has an advantage of disposable usage, which can reduce the fear of the carry-over problems caused by possible adhesion of particles to the channel membrane in FIFFF systems.

This study was supported by the KOSEF (Korea Science & Engineering Foundation) Fund 2005-01858 through the protocol for the scientific and technological cooperation Italy-Korea 2004-2006.

4 References

- Beddeman, T. F., *Environ. Sci. Technol.* 1988, 22, 361–367.
- Ohura, T., Amagai, T., Sugiyama, T., Fusaya, M., Matsushita, H., *Atmos. Environ.* 2004, 38, 2045–2054.
- Ghosal, S., Self, S. A., *Fuel* 1995, 74, 522–529.
- Wiesner, M. R., Grant, M. C., Hutchins, S. R., *Environ. Sci. Technol.* 1996, 30, 3184–3191.
- Grout, H., Tarquis, A. M., Wiesner, M. R., *Environ. Sci. Technol.* 1988, 32, 1176–1182.
- Phillies, G. D. J., *Anal. Chem.* 1990, 62, 1049A–1057A.
- Barth, H. G., Sun, S. T., *Anal. Chem.* 1995, 67, 257R–272R.
- Norton, G. A., Markuszewski, R., Shanks, H. R., *Environ. Sci. Technol.* 1986, 20, 409–413.
- Rincon, J. M., Romero, M., Boccaccini, A. R., *J. Mater. Sci.* 1999, 34, 4413–4423.
- Zhang, Q., Staneier, C. O., Canagaratna, M. R., Jayne, J. *et al.*, *Environ. Sci. Technol.* 2004, 38, 4797–4809.
- Stanier, C. O., Khlystov, A. Y., Pandis, S. N., *Aerosol Sci. Technol.* 2004, 38(S1), 253–264.
- Sakurai, H., Park, K., McMurry, P. H., Zarling, D. D. *et al.*, *Environ. Sci. Technol.* 2003, 37(24), 5487–5495.
- Carlshaf, A., Jönsson, J. A., *J. Chromatogr.* 1988, 461, 89–93.
- Jönsson, J. A., Carlshaf, A., *Anal. Chem.* 1989, 61, 11–18.
- Lee, W. J., Min, B. R., Moon, M. H., *Anal. Chem.* 1999, 71, 3446–3452.
- Min, B. R., Kim, S. K., Ahn, K.-H., Moon, M. H., *J. Chromatogr. A* 2002, 950, 175–182.
- Wijnhoven, J. E. G. J., Koorn, J.-P., Pope, H., Kok, W. Th., *J. Chromatogr.* 1996, 732, 307–315.
- Reschiglian, P., Zattoni, A., Parisi, D., Cinque, L. *et al.*, *Anal. Chem.* 2005, 77, 47–56.
- Kang, D., Moon, M. H., *Anal. Chem.* 2005, 77, 4207–4212.
- Reschiglian, P., Roda, B., Zattoni, A., Min, B., Moon, M. H., *J. Sep. Sci.* 2002, 25, 490–498.
- Reschiglian, P., Zattoni, A., Roda, B., Cinque, L. *et al.*, *J. Chromatogr. A* 2003, 985, 519–529.
- Jensen, K. D., Williams, S. K. R., Giddings, J. C., *J. Chromatogr. A* 1996, 746, 137–145.
- Ratanathanawongs, S. K., Giddings, J. C., *Chromatographia* 1994, 38, 545–554.
- Wahlund, K.-G., Zattoni, A., *Anal. Chem.* 2002, 74, 5621–5628.
- Moon, M. H., Kim, H.-J., Lee, S.-J., Chang, Y.-S., *J. Sep. Sci.* 2005, 28, 1231–1236.
- Giddings, J. C., *Sep. Sci. Technol.* 1985, 20, 749–768.
- Contado, C., Riello, F., Blo, G., Dondi, F., *J. Chromatogr. A* 1999, 845, 303–316.
- Moon, M. H., Kang, D. J., Lee, D. W., Chang, Y. S., *Anal. Chem.* 2001, 73, 693–697.
- Moon, M. H., Kim, H. J., Kwon, S.-Y., Lee, S.-J. *et al.*, *Anal. Chem.* 2004, 76, 3236–3243.
- Moon, M. H., Kang, D. J., Lim, H., Oh, J.-E., Chang, Y.-S., *Environ. Sci. Technol.* 2002, 36, 4416–4423.
- Park, I., Paeng, K.-J., Kang, D., Moon, M. H., *J. Sep. Sci.* 2005, 28, 2043–2049.
- Williams, P. S., Moon, M. H., Giddings, J. C., *Colloids Surf. A* 1996, 113, 215–228.
- Beckett, R., Jiang, Y., Liu, G., Moon, M. H., Giddings, J. C., *Part. Sci. Technol.* 1994, 12, 89–113.
- Giddings, J. C., Moon, M. H., Williams, P. S., Myers, M. N., *Anal. Chem.* 1991, 63, 1366–1372.